Renormalization-group analysis for the infrared properties of a randomly stirred binary fluid

1998 J. Phys. A: Math. Gen. 31 2621

(http://iopscience.iop.org/0305-4470/31/11/012)

J. Phys. A: Math. Gen. **31** (1998) 2621–2637. Printed in the UK PII: S0305-4470(98)82012-X

Renormalization-group analysis for the infrared properties of a randomly stirred binary fluid

Malay K Nandy†§ and Jayanta K Bhattacharjee‡‖

† Institute of Physics, Sachivalaya Marg, Bhubaneswar 751 005, India

‡ Department of Theoretical Physics, Indian Association for the Cultivation of Science, Jadavpur, Calcutta 700 032, India

Received 19 February 1997, in final form 19 August 1997

Abstract. We study the large-scale long-time properties of turbulent motion in a symmetric miscible binary fluid, driven by random stirring fields with correlations $k^{-(d-4+y)}$ and $k^{-(d-2+y')}$ corresponding to the modified Navier–Stokes equation and the convection equation, by means of dynamic renormalization-group (RG) analysis. Unlike the Yakhot–Orszag RG theory, the stability of a fixed point is now determined by *both* the parameters y and y'. Furthermore, the stability now depends on the space dimensionality because of renormalization of the extra coupling, which is a consequence of non-vanishing diagrams in the infrared limit. The Kolmogorov $k^{-5/3}$ spectra, obtained for $y = 4$ and $y' = 2$, is found to be infrared stable against the active dynamics, and corresponds to a stable fixed point with $y > 0$ and $y' < 1.3917y$ in dimension three. The stability condition for the Kolmogorov spectra in infinite dimensions becomes $y' < 1.333y$, differing from the magneto-hydrodynamic case where the Kolmogorov spectrum is only marginally stable in infinite dimensions. There is no other infrared stable fixed point which could be associated with the equipartition ($k^{-3/2}$) spectra of the energies of the velocity and the concentration gradient fields.

1. Introduction

In fully developed hydrodynamic turbulence a wide range of eddy sizes are excited constituting an inertial range of energy cascade where simple phenomenological arguments hold, leading to scaling laws and universal scaling exponents in the inertial range [1, 2]. Similar scaling laws can also be derived in the case of turbulent convection of a passive scalar [3–5]. The dynamical equations, being strongly nonlinear, have been dealt with using renormalized perturbation theories for many years [6–9]. We note that these (Eulerian) theories do not yield the expected (phenomenological) exponents because of a divergence in the small wavenumber region [8], whereas a Lagrangian approach is consistent with the phenomenological exponents [10–12].

The study of the infrared (long wavelength) and long-time properties of a fluid system has been of interest and such a study was first made in the case of a Navier–Stokes fluid (along with the coupled problem of the advection of a passive scalar) by Forster *et al* [13] who modelled the dynamics to be driven by random stirring force fields, through the dynamic renormalization-group (RG) approach of Ma and Mazenko [14]. A generalization of the randomly stirred model was subsequently offered by DeDominicis and Martin [15], in that

§ Present address: Assam University, Silchar, India.

‖ E-mail address: tpjkb@iacs.ernet.in

the Kolmogorov spectrum was obtained for a particular value of a parameter (namely, $y = 4$) coming from the external stirring correlation (the above-mentioned divergence problem does not occur in the RG framework). In particular, these ideas have been found to be useful by Yakhot and Orszag [16] in order to calculate various universal amplitudes associated with high Reynolds number (Kolmogorov) turbulence (including the case of a passive scalar), and they were found to be in remarkable agreement with experimental numbers. We would like to note that the RG analysis and the Eulerian renormalized perturbation theories have been compared, and a remedy to the associated divergence problem has been suggested and self-consistent calculations made within the Eulerian framework [17–21] using ideas borrowed from dynamic critical phenomena [22, 23].

The case of an *active* binary fluid, on the other hand, finds interest as it has relevance to magneto-hydrodynamic fluid systems, differing from the latter by having a scalar order parameter. The turbulence in a symmetric miscible binary fluid has been studied by Ruiz and Nelson [24] phenomenologically as well as numerically by means of employing the eddy-damped quasi-normal Markovian (EDQNM) closure. It has similarity with two-dimensional magneto-hydrodynamic turbulence, which has been studied by Pouquet [25]; the three-dimensional case has been studied by Pouquet *et al* [26]. Kraichnan [10] gave the first phenomenological arguments for the energy transfer process in the magneto-hydrodynamic case.

Ruiz and Nelson [24] found that at large scales (i.e. on the infrared side of wavenumbers) of hydrodynamic fluctuations, the concentration fluctuations (order parameter) behave as a passive scalar. The concentration fluctuations are convected by the turbulent velocity field, the dynamics of the velocity field not being affected by their presence and hence giving rise to the usual Kolmogorov cascade [1, 2] for both the kinetic energy and the mean-square order parameter, with spectra

$$E(k) \sim \bar{\varepsilon}^{2/3} k^{-5/3} \qquad C(k) \sim \bar{N} \bar{\varepsilon}^{-1/3} k^{-5/3} \tag{1}$$

where $\bar{\varepsilon}$ and $\bar{N}$ are energy and mean square scalar injection rates into the fluid at some macroscopic scale and k is the inverse length scale; $E(k)$ and $C(k)$ are the densities of the energy and mean-square scalar between k and $k + \mathrm{d}k$.

However, when the mixing by means of this cascade process has sufficiently taken place, and has reached some small scale (on the ultraviolet side of the wavenumbers), i.e. after a sufficient build-up of concentration gradients, the two components begin to 'see' each other, and a new term in the Navier–Stokes equation begins to become important. This term starts to take (active) part in determining the dynamics of the velocity field. Correspondingly, there is a cross-over wavenumber k_c; in the range $k < k_\mathrm{c}$, there occurs the usual Kolmogorov cascade with spectra given by equation (1), while in the range $k > k_\mathrm{c}$, the scaling laws are expected to be different.

The situation in the ultraviolet (UV) range $k > k_\mathrm{c}$ is then similar to that of magneto-hydrodynamic (MHD) turbulence, where, as Kraichnan argues [10], the inertial range (Kolmogorov) phenomenology has to be modified, because the presence of a large-scale magnetic field $\boldsymbol{B}_0$ now affects the energy transfer (unlike the Kolmogorov phenomenology, where the energy transfer is *not* affected by a uniform convection). This gives rise to oppositely propagating Alfvén waves along $\boldsymbol{B}_0$ corresponding to the fields $(\boldsymbol{u} + \boldsymbol{b})$ and $(\boldsymbol{u} - \boldsymbol{b})$ ($\boldsymbol{b}$ being the turbulent small-scale magnetic field, and $\boldsymbol{u}$ the velocity field), each moving with speed B_0. Energy-cascade results from scattering between these waves. The time-scale associated with such scattering is given by $\theta_k \sim 1/B_0 k$ (while that with the kinetic motion is $\tau_k \sim 1/v_k k$, v_k being the Kolmogorovian velocity scale).

Furthermore, Kraichnan arrived at another conclusion [10]. The relative distortion factor due to the Alfvénic scattering (by which the Kolmogorovian energy transfer rate is reduced) is given by

$$\frac{\theta_k}{\tau_k} \sim \frac{v_k}{B_0} \ll 1 \tag{2}$$

assuming the total kinetic energy of the fluid to be very small compared to B_0^2. This suggests weak scattering, and hence almost freely propagating Alfvén waves. Consequently, this implies weak correlation between the $(\boldsymbol{u}+\boldsymbol{b})$ and $(\boldsymbol{u}-\boldsymbol{b})$ fields, leading to asymptotic equipartition of the energies of the $\boldsymbol{u}$ and $\boldsymbol{b}$ fields.

The phenomenological derivation of the energy spectrum in this equipartition range, due to Kraichnan [10], rests on the assumption of localness of interactions. The energy transfer rate $\Pi(k) = \bar{\varepsilon}$ should be proportional to θ_k, since $\theta_k \ll \tau_k$. Furthermore, $\Pi(k)$ may depend only on the inertial range quantities k and $E(k)$. Assuming $\Pi(k) = \bar{\varepsilon} \sim \theta_k k^{\alpha}[E(k)]^{\beta}$, and noting that $[\bar{\varepsilon}] = [L^2T^{-3}]$ and $[E(k)] = [L^3T^{-2}]$, leads to $-\alpha + 3\beta = 2$ and $1 - 2\beta = -3$, yielding $\alpha = 4$ and $\beta = 2$; hence

$$E(k) \sim (\bar{\varepsilon} B_0)^{1/2} k^{-3/2}. \tag{3}$$

Ruiz and Nelson [24] noted that the above MHD phenomenology should be applicable to the UV wavenumbers $k > k_{\mathrm{c}}$ in the case of a turbulent binary fluid, with the root-mean-square gradient

$$B_{\mathrm{c}} = (\langle|\nabla\psi|^2\rangle)^{1/2} = \left(\int_0^{k_{\mathrm{c}}} k^2 C(k)\,\mathrm{d}k\right)^{1/2} \tag{4}$$

due to the Kolmogorov range interpreted as the counterpart of the magnetic field B_0.

Correspondingly, Ruiz and Nelson argued that Alfvén-like waves would be important in this UV regime, which gives rise to an equipartition between the energies of the velocity and concentration gradient fields, yielding the spectrum

$$E(k) = 2\alpha_0 k^2 C(k) \sim (\bar{\varepsilon} B_{\mathrm{c}})^{1/2} k^{-3/2}. \tag{5}$$

This spectrum is consistent with the EDQNM closure, with the inverse Alfvénic time scale $\omega(k) \sim \sqrt{\alpha_0} B_{\mathrm{c}} k$.

An estimate about the cross-over wavenumber k_{c} can be obtained by noting that the Kolmogorov time scale, given by the inverse of $\eta(k) \sim \bar{\varepsilon}^{1/3} k^{2/3}$, should catch up with the Alfvénic time scale at this wave number, i.e. $\eta(k_{\mathrm{c}}) = \omega(k_{\mathrm{c}})$, giving $k_{\mathrm{c}} \sim \bar{\varepsilon}/\alpha_0^{3/2} B_{\mathrm{c}}^3$. Noting that $B_{\mathrm{c}} \sim \bar{N}^{1/2} \bar{\varepsilon}^{-1/6} k_{\mathrm{c}}^{2/3}$, we obtain $k_{\mathrm{c}} \sim (\bar{\varepsilon}/\alpha_0 \bar{N})^{1/2}$.

Here we intend to analyse the large-wavelength and long-time properties of a symmetric binary fluid driven by random stirring force fields employing the dynamic RG approach as cited above [13, 14, 16]. Having an extra nonlinearity in the Navier–Stokes dynamics, the active participation of the order parameter is expected to affect the passive regimes including the stability of the Kolmogorov regime. Furthermore, the binary fluid case, having a scalar order parameter, would be interesting for the purpose of comparison with the MHD case. The magnetic potential is a vector for any general dimension $d \geqslant 2$; carrying out the RG analysis for a general d would then be interesting for the purpose of comparison with the MHD case—the RG studies for the MHD case have already been made by Fournier *et al* [27]. We find, unlike in the passive scalar case, that the stability of the passive regime IR fixed points (against the active participation of concentration fluctuations) depends on the nature of both the stirring fields associated with the modified Navier–Stokes and the advection dynamics. The nature of these stabilities differs from that in the MHD case. The Kolmogorov spectra correspond to a fixed point which is stable in the IR limit against the active participation of the concentration fluctuations. There is no other stable fixed point in the IR limit which could be associated with the equipartition spectra.

We need to comment on the nature of our calculation. We ignore the fluctuations in the energy transport—this is the Kolmogorov assumption and is reasonable for low-order structure factors. Thus, one is saddled with a mean-field calculation—but in the mean-field version there can be two distinct attitudes. One is to go the Mou–Weichmann [28] way and cast the mean-field theory as a spherical limit; in that case one does not obtain the Kolmogorov spectrum ($E(k) \propto k^{-3/2}$ instead). The other is to use the Yakhot–Orszag [16] prescription with the understanding that the sweeping effect of the large eddies has been explicitly removed [19]. We opt for the latter attitude bearing in mind that the Kolmogorov law $E(k) \propto k^{-5/3}$ is almost always fairly close to experimental values.

We end by noting a feature that the RG arguments cannot capture. Neglecting dissipation and forcing, the equations of motion admit a steady-state solution where the expectation value of the square of the velocity is a constant and the square of the order parameter ψ^2 has an average value $\langle\psi^2\rangle = (A + Bk^2)^{-1}$. Active coupling corresponds to $B \neq 0$ and passive coupling to $B = 0$. For passive coupling the expectation values of both v^2 and ψ^2 are constant and the spectra are weighted towards high k, leading to the usual UV cascade. For active coupling with $B \neq 0$, it is possible to have A small and negative, in which case a concentration pile up would occur at $k_0^2 = -A/B$. If injection occurs at $k > k_0$, there can be an inverse cascade of the concentration field.

2. The randomly stirred model

The turbulent hydrodynamics of an incompressible symmetric binary fluid can be modelled as [24]

$$\frac{\partial \boldsymbol{u}}{\partial t} + (\boldsymbol{u}\cdot\nabla)\boldsymbol{u} = -\frac{\nabla P}{\rho_0} - \alpha_0 \nabla\psi\nabla^2\psi + \nu_0\nabla^2\boldsymbol{u} + \boldsymbol{f} \tag{6}$$

$$\frac{\partial \psi}{\partial t} + (\boldsymbol{u}\cdot\nabla)\psi = \mu_0\nabla^2\psi + \theta \tag{7}$$

along with the incompressibility condition

$$\nabla\cdot\boldsymbol{u} = 0 \tag{8}$$

where $\boldsymbol{u}(\boldsymbol{x}, t)$ and $P(\boldsymbol{x}, t)$ are the velocity and pressure fields, respectively, and

$$\psi(\boldsymbol{x}, t) = \frac{\rho_A(\boldsymbol{x}, t) - \rho_B(\boldsymbol{x}, t)}{\rho_0}$$

is the concentration field (order parameter), with $\rho_A(\boldsymbol{x}, t)$ and $\rho_B(\boldsymbol{x}, t)$ the density fields of the two compounds A and B, and ρ_0 the mean density. Here ν_0 is the kinematic viscosity of the binary fluid and μ_0 the molecular diffusivity of the order parameter.

In the above equations both the velocity and the concentration fields are modelled as being driven by the random stirring force fields $\boldsymbol{f}(\boldsymbol{x}, t)$ and $\theta(\boldsymbol{x}, t)$, which will be assumed to have Gaussian statistics.

Equation (6) clearly shows an extra term (involving α_0), which determines the effect of the concentration field on the dynamics of the velocity field. Because of the presence of multiple space derivatives, this term is negligible compared to the convection term on the left-hand side at large scales, whence the dynamics can be approximated by that of a passive scalar ($\alpha_0 = 0$). This term becomes important only at small scales, when we can no longer neglect its effect.

As a consequence, the perturbative RG treatment of this problem involves many extra diagrams along with those of Forster *et al* [13] or Yakhot and Orszag [16], giving rise to a very complicated RG analysis.

2.1. Fourier transforms

We introduce the Fourier transforms of the fields as

$$\boldsymbol{u}(\boldsymbol{x}, t) = \int \frac{\mathrm{d}^d \boldsymbol{k}\, \mathrm{d}\omega}{[2\pi]^{d+1}} \boldsymbol{u}(\boldsymbol{k}, \omega)\, \mathrm{e}^{\boldsymbol{k}\cdot\boldsymbol{x}-\omega t} \tag{9}$$

$$\psi(\boldsymbol{x}, t) = \int \frac{\mathrm{d}^d \boldsymbol{k}\, \mathrm{d}\omega}{[2\pi]^{d+1}} \psi(\boldsymbol{k}, \omega)\, \mathrm{e}^{\boldsymbol{k}\cdot\boldsymbol{x}-\omega t} \tag{10}$$

where a UV cut-off at Λ to the k-integration, corresponding to the 'internal' cut-off (viscous or diffusive, whichever is smaller) is assumed. We also assume similar Fourier transforms for the driving fields $\boldsymbol{f}(\boldsymbol{x}, t)$ and $\theta(\boldsymbol{x}, t)$, and the pressure field $P(\boldsymbol{x}, t)$. Equations (6) and (7) can then be written as

$$(-\mathrm{i}\omega + \nu_0 k^2) u_i(\boldsymbol{k}, \omega) = f_i(\boldsymbol{k}, \omega) - \frac{\mathrm{i}\lambda_0}{2} P_{ijl}(\boldsymbol{k}) \int \frac{\mathrm{d}^d \boldsymbol{p}\, \mathrm{d}\omega}{[2\pi]^{d+1}} u_j(\boldsymbol{p}, \omega') u_l(\boldsymbol{q}, \omega'')$$
$$+ \frac{\mathrm{i}\alpha_0}{2} P_{ij}(\boldsymbol{k}) \int \frac{\mathrm{d}^d \boldsymbol{p}\, \mathrm{d}\omega'}{[2\pi]^{d+1}} (p^2 q_j + q^2 p_j) \psi(\boldsymbol{p}, \omega') \psi(\boldsymbol{q}, \omega'') \tag{11}$$

and

$$(-\mathrm{i}\omega + \mu_0 k^2) \psi(\boldsymbol{k}, \omega) = \theta(\boldsymbol{k}, \omega) - \mathrm{i}\bar{\lambda}_0 \int \frac{\mathrm{d}^d \boldsymbol{p}\, \mathrm{d}\omega'}{[2\pi]^{d+1}} q_j u_j(\boldsymbol{p}, \omega') \psi(\boldsymbol{q}, \omega'') \tag{12}$$

with $q = |\boldsymbol{k} - \boldsymbol{p}|$ and $\omega'' = \omega - \omega'$. The incompressibility condition becomes

$$k_j u_j(\boldsymbol{k}, \omega) = 0. \tag{13}$$

In the above we have introduced the formal parameter λ_0 and $\bar{\lambda}_0 (= 1)$ in order to construct perturbation expansions in powers of λ_0 and $\bar{\lambda}_0$ (and also α_0).

2.2. Non-equilibrium model

We shall assume that the external driving fields have Gaussian white noise statistics, with correlations

$$\langle f_i(\boldsymbol{k}, \omega) f_i(\boldsymbol{k}', \omega') \rangle = F(k) P_{ij}(\boldsymbol{k}) [2\pi]^d \delta^d(\boldsymbol{k} + \boldsymbol{k}') [2\pi] \delta(\omega + \omega') \tag{14}$$

and

$$\langle \theta(\boldsymbol{k}, \omega) \theta(\boldsymbol{k}', \omega') \rangle = \Theta(k) [2\pi]^d \delta^d(\boldsymbol{k} + \boldsymbol{k}') [2\pi] \delta(\omega + \omega'). \tag{15}$$

The model we shall study is

$$F(k) = \frac{2D_0}{k^s} \qquad \text{and} \qquad \Theta(k) = \frac{2\mathcal{D}_0}{k^{s'}} \tag{16}$$

with $s > -2$ and $s' > -2$. The cases $s = -2$ and $s' = -2$ correspond to equilibrium where fluctuation–dissipation theorems hold.

The noise added in the concentration field equation of motion is meant to facilitate the calculation of correlation functions. The variation $k^{-s'}$ in the noise strength is taken to ensure the fact that the Kolmogorov spectrum for the velocity field will be obtained even in the presence of the active dynamics. It will be seen that Kolmogorov's result follows if we take $s = s' = D$.

3. Perturbative RG

The RG treatment consists of eliminating modes $\boldsymbol{u}^{>}(\boldsymbol{k},\omega)$ and $\psi^{>}(\boldsymbol{k},\omega)$ from thin shells of wavenumbers (belonging to $\Lambda\,\mathrm{e}^{-r} < k < \Lambda$) starting from the UV end, by means of integrating away these modes. The corresponding effect on the IR modes $\boldsymbol{u}^{<}(\boldsymbol{k},\omega)$ and $\psi^{<}(\boldsymbol{k},\omega)$ (belonging to $0 < k < \Lambda\,\mathrm{e}^{-r}$) is then reflected through an augmentation in the transport constants ν_0 and μ_0, and the coupling constant α_0. (The coupling constant λ_0, however, does not undergo any relevant correction due to such an elimination process, a consequence of Galelian invariance [13].) This elimination process is repeated in recursive steps (or infinitesimal r), so that we may expect to approach a (stable) fixed point after many such infinitesimal steps, i.e. in the IR limit $k \to 0$.

The recursion relations are found by standard diagrammatic perturbation theory (see figures 1–6). We write down the answers in what follows. The additional linear terms generated in equation (11) and (12) after mode elimination are (considering only the passive dynamics)

$$G_0(k,\omega)\left[-A_d\frac{\lambda_0^2 D_0}{\nu_0^2}\left(\frac{\mathrm{e}^{yr}-1}{y\Lambda^y}\right)k^2 u_i^{<}(\boldsymbol{k},\omega)\right]$$

and

$$\mathcal{G}_0(k,\omega)\left[-B_d\frac{\lambda_0^2 D_0}{\nu_0(\nu_0+\mu_0)}\left(\frac{\mathrm{e}^{yr}-1}{y\Lambda^y}\right)k^2\psi^{<}(\boldsymbol{k},\omega)\right].$$

The corresponding contributions from active dynamics are

$$G_0(k,\omega)\left[-M_d\frac{\alpha_0\bar{\lambda}_0\mathcal{D}_0}{\mu_0^2}\left(\frac{\mathrm{e}^{y'r}-1}{y'\Lambda^{y'}}\right)k^2\right]u_i^{<}(\boldsymbol{k},\omega)$$

and

$$\mathcal{G}_0(k,\omega)\left[N_d\frac{\alpha_0\bar{\lambda}_0\mathcal{D}_0}{\mu_0(\mu_0+\nu_0)}\left(\frac{\mathrm{e}^{y'r}-1}{y'\Lambda^{y'}}\right)k^2\right]\psi^{<}(\boldsymbol{k},\omega).$$

Consequently the corrections to the bare viscosity and diffusivity are

$$\Delta\nu(0,0) = A_d\frac{\lambda_0^2 D_0}{\nu_0^2}\left(\frac{\mathrm{e}^{yr}-1}{y\Lambda^y}\right) + M_d\frac{\alpha_0\lambda_0\mathcal{D}_0}{\mu_0^2}\left(\frac{\mathrm{e}^{y'r}-1}{y'\Lambda^{y'}}\right) \tag{17}$$

$$\Delta\mu(0,0) = B_d\frac{\bar{\lambda}_0^2 D_0}{\nu_0(\nu_0+\mu_0)}\left(\frac{\mathrm{e}^{yr}-1}{y\Lambda^y}\right) - N_d\frac{\alpha_0\bar{\lambda}_0\mathcal{D}_0}{\mu_0(\mu_0+\nu_0)}\left(\frac{\mathrm{e}^{y'r}-1}{y'\Lambda^{y'}}\right) \tag{18}$$

where

$$s = d-4+y \tag{19a}$$

$$A_d = \frac{S_d}{(2\pi)^d}\frac{d^2-d-y}{2d(d+2)} \tag{19b}$$

$$B_d = \frac{S_d}{(2\pi)^d}\frac{d-1}{d} \tag{19c}$$

$$s' = d-2+y' \tag{19d}$$

$$M_d = \frac{S_d}{(2\pi)^d}\frac{d+y'}{2d(d+2)} \tag{19e}$$

$$N_d = B_d. \tag{19f}$$

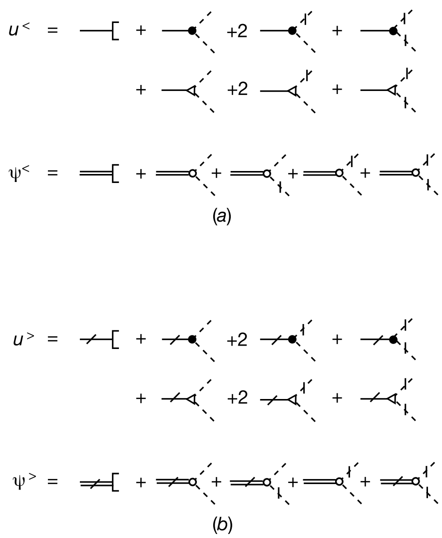

Figure 1. Diagrammatic equations (a) for $u^<$ and $\psi^<$, and (b) for $u^>$ and $\psi^>$. The full single and double lines represent the bare velocity and scalar propagators $G^{(0)}$ and $\mathcal{G}^{(0)}$; the dashed lines correspond to the velocity and scalar fields $u_i^{(0)}$ and $\psi^{(0)}$.

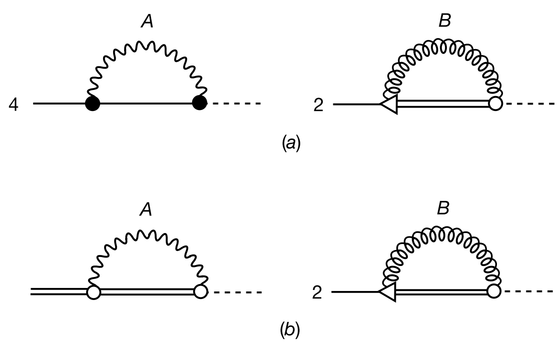

Figure 2. Loop diagrams representing (a) the correction to the bare 'viscosity' $\nu_0 k^2$ and (b) correction to the bare 'diffusivity' $\mu_0 k^2$. The wavy and curly lines represent the velocity and scalar correlations, respectively.

4. Noise renormalization

Forster *et al* [13] and Yakhot and Orszag [16] calculated the one-loop correction

$$Q_{ij}^{(2)A}(k;k') = \langle u_i^{(1)A}(k) u_j^{(1)A}(k')\rangle \tag{20}$$

the first loop-diagram in figure 3(a), which is a correction to the correlation

$$Q_{ij}^{(0)}(k;k') = Q^{(0)}(k) P_{ij}(\boldsymbol{k})(2\pi)^{d+1}\delta^{d+1}(k+k') \tag{21}$$

where $Q^{(0)}(k) = |G_0(k)|^2 F(k)$, with $F(k) = 2D_0/k^s$. The corresponding correction to D_0, in the limit $k \to 0$ and $\omega \to 0$, was found to be

$$\Delta D^A(k,0) = Q_d \frac{\lambda_0^2 D_0^2}{2\nu_0^3} k^{2+s} \frac{e^{(6+2s-d)r} - 1}{(6+2s-d)\Lambda^{6+2s-d}} \tag{22}$$

with

$$Q_d = \frac{S_d}{[2\pi]^d}\frac{d^2-2}{d(d+2)}.$$

Clearly ΔD^A adds a k-independent, and hence relevant, correction to the constant D_0 only when $s = -2$. In terms of the small parameter y (given by $s = d - 4 + y$) the above correction becomes

$$\Delta D^A(k,0) = Q_d \frac{\lambda_0^2 D_0^2}{2\nu_0^3} k^{d-2+y} \frac{\mathrm{c}^{(d-2+2y)r} - 1}{(d-2+2y)\Lambda^{d-2+2y}} \tag{23}$$

so that the condition of relevant correction becomes $y = 2 - d$. Thus, when $s = -2$ or $y = 2 - d$, the constant correction to D_0 becomes

$$\Delta D^A(0,0) = Q_d \frac{\lambda_0^2 D_0^2}{2\nu_0^3} \frac{\mathrm{e}^{(2-d)r} - 1}{(2-d)\Lambda^{2-d}} \tag{24}$$

which is the case for model A of Forster *et al* [13].

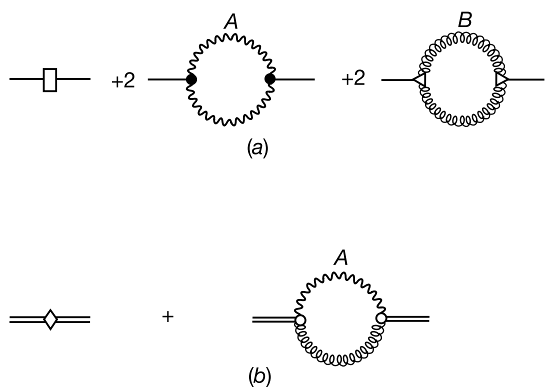

Figure 3. Corrected velocity and scalar correlations. (a) Diagrams for $Q_{ij}^{(0)}(\boldsymbol{k},\omega)$, $Q_{ij}^{(2)A}(\boldsymbol{k},\omega)$ and $Q_{ij}^{(2)B}(\boldsymbol{k},\omega)$. The two loops add the correction to the force correlation $F(k)$, represented by the square in the first diagram. (b) Diagrams for $\Phi^{(0)}(\boldsymbol{k},\omega)$ and $\Phi^{(2)A}(\boldsymbol{k},\omega)$. The two loops add the correction to the noise correlation $\Theta(k)$, represented by the diamond in the first diagram.

Furthermore, for any $s > -2$ or $y > 2 - d$, ΔD^A is proportional to a positive power of k, and hence becomes irrelevant, for it then goes to zero in the RG limit $k \to 0$. In the present analysis, we shall consider only this (non-equilibrium) case.

Because of the active coupling α_0 term, in addition to the above, there is another correction to D_0, obtained from the one-loop correlation

$$Q_{ij}^{(2)B}(k;k') = \langle u_i^{(1)B}(k) u_j^{(1)B}(k')\rangle$$

represented by the second loop diagram in figure 3(a). The corresponding correction ΔD^B is found to be (we do not present the calculation here)

$$\Delta D^B(k,0) = \frac{1}{2} P_d \frac{f_0^2}{g_0}\frac{\mu_0}{\nu_0}\Lambda^{2s'-s-d} k^{2+s} \frac{\mathrm{e}^{(2+2s'-d)r} - 1}{(2+2s'-d)} \tag{25}$$

in terms of the modified couplings

$$g_0 = \frac{\lambda_0^2 D_0}{\nu_0^3 \Lambda^{4-d+s}} \qquad \text{and} \qquad f_0 = \frac{\alpha_0 \lambda_0 \mathcal{D}_0}{\mu_0^2 \nu_0 \Lambda^{2-d+s'}}$$

and

$$P_d = \frac{S_d}{[2\pi]^d}\frac{2}{d(d+2)}.$$

Again, this correction becomes relevant when $s = -2$ or $y = 2-d$. However, the presence of a power of Λ complicates the situation, which would lead to breakdown of scaling. It is to be noted that, for $s = -2$, there is no power of Λ only when $d = 2 + 2s'$, whereas for the special case $s' \neq 0$ the small parameter is $(2-d)$ as it was for the correction ΔD^A, so therefore a factor Λ^{2-d} remains. However, since we are interested in the non-equilibrium case $s > -2$ (or $y > 2-d$), this correction becomes irrelevant for our purpose.

Next, there is the correction given by the loop in figure 3(b)

$$\Phi^{(2)A}(k; k') = \langle \psi^{(1)A}(k)\psi^{(1)A}(k')\rangle$$

to the correlation of the concentration field, namely

$$\Phi^{(0)}(k; k') = \Phi^{(0)}(k)(2\pi)^4\delta^4(k + k')$$

where $\Phi^{(0)}(k) = |\mathcal{G}_0(k)|^2\Theta(k)$, with $\Theta(k) = 2\mathcal{D}_0/k^{s'}$. The corresponding correction to $\mathcal{D}_0$, in the limit $k \to 0$ and $\omega \to 0$, can be found to be

$$\Delta\mathcal{D}^A(k, 0) = B_d \frac{\bar{\lambda}_0^2 D_0 \mathcal{D}_0}{\nu_0\mu_0(\nu_0 + \mu_0)} k^{2+s'} \frac{e^{(6+s+s'-d)r} - 1}{(6 + s + s' - d)\Lambda^{6+s+s'-d}} \tag{26}$$

which clearly is a k-independent (i.e. relevant) correction to $\mathcal{D}_0$ for $s' = -2$, or if we use $s' = d - 2 + y'$, then $y' = -d$. This latter relation is quite unlike the MHD case. This difference is attributed to the fact that here the convected quantity ψ is a scalar. For any $s' > -2$ or $y' > -d$, this correction becomes irrelevant.

5. Vertex renormalization

The lowest-order vertex correction diagrams are given in figures 4–6. The correction to the bare couplings λ_0 and $\bar{\lambda}_0$, one in the Navier–Stokes equation and the other in the convection equation, vanish in the IR limit, which is necessarily a consequence of Galelian invariance of the equations of motion; see [24].

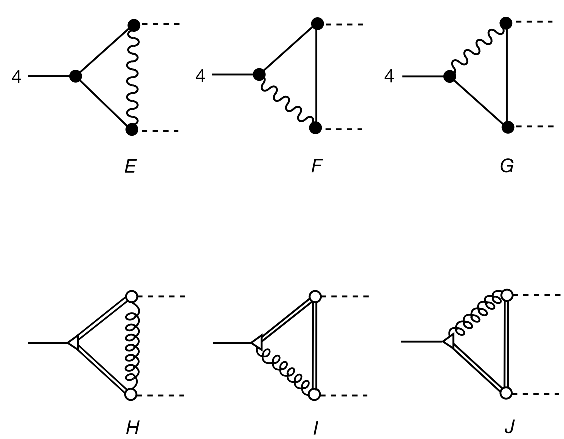

Figure 4. One-loop corrections to the λ_0-vertex.

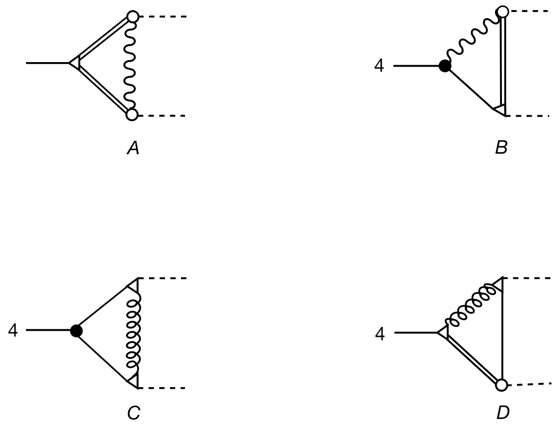

Figure 5. One-loop corrections to the α_0-vertex.

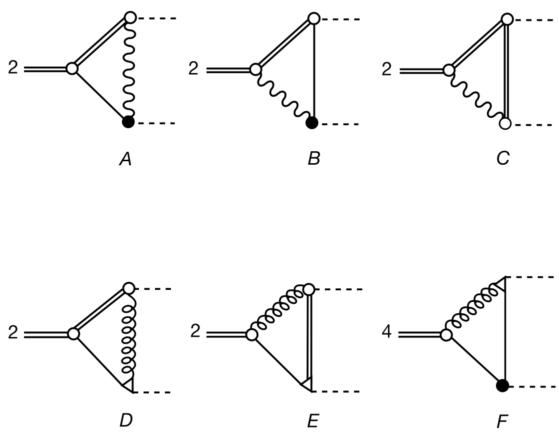

Figure 6. One-loop corrections to the $\bar{\lambda}_0$-vertex.

However, the correction to α_0 due to the loop diagrams in figure 5 do not vanish in the IR limit; there is no known invariance principle that would make such renormalization vanish.

These diagrams can be evaluated by restricting the internal wavenumbers in the range $\Lambda\,\mathrm{e}^{-r} < p < \Lambda$, and using a similar procedure as we have just used to evaluate the corrections to viscosity and diffusivity. Since the calculations are long and tedious, we shall only present the final results:

$$\Delta\alpha^A(0,0) = -P_d \frac{\alpha_0\lambda_0^2 D_0}{\nu_0\mu_0(\nu_0+\mu_0)}\left(\frac{\mathrm{e}^{yr}-1}{y\Lambda^y}\right) \tag{27a}$$

$$\Delta\alpha^B(0,0) = -Q_d \frac{\alpha_0\lambda_0^2 D_0}{\nu_0^2(\nu_0+\mu_0)}\left(\frac{\mathrm{e}^{yr}-1}{y\Lambda^y}\right) \tag{27b}$$

$$\Delta\alpha^C(0,0) = Q_d \frac{\alpha_0^2\lambda_0 \mathcal{D}_0}{\nu_0\mu_0(\nu_0+\mu_0)}\left(\frac{\mathrm{e}^{y'r}-1}{y'\Lambda^{y'}}\right) \tag{27c}$$

$$\Delta\alpha^D(0,0) = P_d \frac{\alpha_0^2\lambda_0 \mathcal{D}_0}{\mu_0^2(\nu_0+\mu_0)}\left(\frac{\mathrm{e}^{y'r}-1}{y'\Lambda^{y'}}\right) \tag{27d}$$

where the superscripts refer to the diagrams $A \ldots D$ in figure 5, and the arguments (0,0) refer to the zero external wavenumber and frequency limit. The right-hand sides being k-independent, these corrections become relevant in this RG limit.

6. Flow equations

Now we assume that the RG analysis is iterated in infinitesimal steps of r, so that we expand the recursion relations in the limit $r \to 0$. Using equations (17), (18), (23), (25), (26), (27a–27d), and expanding about $r = 0$, we get, after assuming the iterative nature of the RG method,

$$\frac{\mathrm{d}\nu}{\mathrm{d}r} = \nu(r)[-2 + z(r) + A_d g(r) + M_d f(r)] \tag{28}$$

$$\frac{\mathrm{d}\mu}{\mathrm{d}r} = \mu(r)\left[-2 + z(r) + B_d \frac{g(r)}{\kappa(r)[1+\kappa(r)]} - N_d \frac{f(r)}{1+\kappa(r)}\right] \tag{29}$$

$$\frac{\mathrm{d}\lambda}{\mathrm{d}r} = \lambda(r)\left[-3 + \frac{y}{2} + \frac{3}{2}z(r)\right] \tag{30}$$

$$\frac{\mathrm{d}\alpha}{\mathrm{d}r} = \alpha(r)\Bigg[-3 - \frac{y}{2} + y' + \frac{3}{2}z(r) - \{P_d + Q_d\kappa(r)\}\frac{g(r)}{\kappa(r)[1+\kappa(r)]} + \{P_d + Q_d\kappa(r)\}\frac{f(r)}{1+\kappa(r)}\Bigg] \tag{31}$$

where $z(r)$ is the factor for frequency rescaling, and r is no longer an infinitesimal argument. In the above equations, we have defined the scaled couplings as

$$g(r) = \frac{D_0}{\Lambda^y}\frac{\lambda^2(r)}{\nu^3(r)} \qquad f(r) = \frac{\mathcal{D}_0}{\Lambda^{y'}}\frac{\alpha(r)\lambda(r)}{\mu^2(r)\nu(r)} \qquad \kappa(r) = \frac{\mu(r)}{\nu(r)} \tag{32}$$

which are similar to the definitions for the corresponding bare quantities. Although the flow equations in equations (28)–(31) depend on $z(r)$, the corresponding equations for the new couplings given by equation (32) do not. Differentiating these definitions with respect to r and using equations (28)–(31) we get the following flow equations:

$$\frac{\mathrm{d}g}{\mathrm{d}r} = g(r)[y - 3A_d g - 3M_d f] \tag{33}$$

$$\frac{\mathrm{d}f}{\mathrm{d}r} = f(r)\left[y' - \{2B_d + P_d + Q_d\kappa\}\frac{g}{\kappa(1+\kappa)} - A_d g + \{2N_d + P_d + Q_d\kappa\}\frac{f}{1+\kappa} - M_d f\right] \tag{34}$$

$$\frac{\mathrm{d}\kappa}{\mathrm{d}r} = \kappa(r)\left[B_d\frac{g}{\kappa(1+\kappa)} - A_d g - N_d\frac{f}{1+\kappa} - M_d f\right] \tag{35}$$

where we have suppressed the argument r for brevity.

7. Fixed points of active dynamics

An analysis of the RG flow equations of the previous section can easily be performed with the idea of a fixed point, without solving the flow equations exactly. We assume that as the RG iteration is carried out, i.e. as $r \to \infty$, the scaled coupling constants $g(r)$, $\kappa(r)$ approach a set of constant values, called a fixed point, i.e. they cease to be r-dependent after infinitely many steps of RG iterations, so that the right-hand sides of equations (33)–(35) tend to zero as one approaches the fixed point. However, the right-hand sides can be zero at more than one point. The existence of a fixed point depends on its (linear) stability with respect to infinitesimal perturbations around that point. For a passive scalar this stability depends only on the sign of y but *not* on the parameter y' [13, 16].

However, we directly go over to the case of convection of an active scalar. The corresponding fixed points are obtained from equations (33)–(35). Unlike the passive-scalar case, we shall find that the stability of the fixed points now depends on *both* the parameters y and y'.

7.1. Passive regime (affected by the active dynamics)

Case I. $y > 0$. We shall investigate the behaviour of the fixed point

$$g \to g^* \qquad \kappa \to \kappa^* \qquad f \to 0 \tag{36}$$

where g^* and κ^* are non-zero. This fixed point includes the scaling laws for the Kolmogorov cascade of both energy and the (passive) scalar invariance $\langle \psi^2 \rangle$, hence the name passive regime.

From equations (33)–(35), we then have

$$y - 3A_d g^* = 0 \tag{37}$$

$$B_d \frac{g^*}{\kappa^*(1+\kappa^*)} - A_d g^* = 0 \tag{38}$$

so that

$$g^* = \frac{y}{3A_d(0)} + \mathrm{O}(y^2) \tag{39}$$

$$\kappa^* = \frac{1}{2}\left[-1 + \sqrt{1 + \frac{8(d+2)}{d}}\right] + \mathrm{O}(y) \tag{40}$$

where we have used the expressions for $A_d(y)$ and B_d and performed a y-expansion. These results are in agreement with those of [16].

Stability. We observe that the above fixed point is similar to that of Yakhot and Orszag, because the extra coupling, which is not present in Yakhot–Orszag theory, goes to zero. The stability of the Yakhot–Orszag fixed point does not depend on the value of y', the parameter coming from the scalar-stirring correlation. However, now, because of the presence of the extra coupling $f(r)$, the stability of the present fixed point does depend on the values of y'.

To investigate its stability, we assume

$$g(r) = g^* + \delta g \qquad \kappa(r) = \kappa^* + \delta\kappa \qquad f(r) = 0 + \delta f \tag{41}$$

where δg, $\delta\kappa$, and δf are infinitesimal perturbations. Substituting them in equations (33)–(35), and retaining only first-order terms, we obtain the stability matrix as

$$\frac{\mathrm{d}}{\mathrm{d}r}\begin{pmatrix}\delta g\\ \delta\kappa\\ \delta f\end{pmatrix} = \begin{pmatrix} -y & 0 & -y\frac{M_d}{A_d} \\ 0 & -\frac{y}{3}\left(\frac{1+2\kappa^*}{1+\kappa^*}\right) & -\left(\frac{N_d}{1+\kappa^*} + M_d\right)\kappa^* \\ 0 & 0 & y' - \left(1 + \frac{P_d + Q_d\kappa^*}{3B_d}\right) y \end{pmatrix}\begin{pmatrix}\delta g\\ \delta\kappa\\ \delta f\end{pmatrix}. \tag{42}$$

For stability, the eigenvalues of this matrix, which are just its diagonal elements, must be negative. Since κ^* is positive, we must therefore have y positive. Furthermore, we must also have

$$y' < a_d y \qquad \text{with } y > 0 \tag{43}$$

where

$$a_d = \left(1 + \frac{P_d + Q_d\kappa^*}{3B_d}\right) = \left(1 + \frac{2 + (d^2-2)\kappa^*}{3(d-1)(d+2)}\right).$$

Thus for $d = 3$ we have $a_3 = 1.3917$, and the condition of stability for the passive regime becomes $y' < 1.3917y$ with $y > 0$.

In the infinite-dimensional limit, we have $\kappa^* = 1$ and hence $a_\infty = 1.333$, leading to the stability criterion $y' < 1.333y$. This situation is quite unlike the MHD case [27], where $a_\infty = 1$, the stability condition being $y' < y$.

However, (artificially) suppressing the renormalization of the active vertex α_0 amounts to setting $P_d = Q_d = 0$. Then the stability condition, similar to the MHD case, becomes $y' < y$, independent of the dimensionality d.

Case II. $y = 0$. We consider the fixed point $(g, f, \kappa) = (0, 0, \kappa^*)$, with κ^* a non-zero quantity. Considering a small perturbation about this point, we find from equation (34) that $\mathrm{d}(\delta f)/\mathrm{d}r \approx y'\delta f$, leading to $\delta f \approx \mathrm{e}^{y'r}$. Clearly, the stability requires $y' < 0$.

Furthermore, from equation (33), the solution $\delta g(r) \sim 1/r$ approaches zero at a much slower rate than an exponential. As a consequence (as the previous exact results [13, 16] would suggest), the right-hand side of equation (35) approaches zero by virtue of the quick approach of $f(r)$ towards zero (while $g(r)$ approaches zero too slowly) only when κ approaches κ^* as quickly (or quicker than the approach of $g(r)$), given by equation (38) leading to the universality similar to the MHD case [27].

Case III. $y < 0$. We consider a similar fixed point, $(g, f, \kappa) = (0, 0, \kappa')$, as the previous case. However, since y is now non-zero, considering small perturbations leads to $\mathrm{d}(\delta g)/\mathrm{d}r \approx y\delta g$, and $\mathrm{d}(\delta f)/\mathrm{d}r \approx y'\delta f$, giving $\delta g \sim \mathrm{e}^{yr}$ and $\delta f \sim \mathrm{e}^{y'r}$. Clearly it is unstable when $y > 0$ and $y' > 0$, and stable (i.e. exists) only when $y < 0$ and $y' < 0$ simultaneously.

Since $g(r)$ and $f(r)$ both approach zero exponentially in this case, presumably much quicker than how κ approaches κ^*, the right-hand side of equation (35) approaches zero by virtue of the quick approaches of $g(r)$ and $f(r)$ towards zero. This, presumably, leads to the break of universality (making values of κ' depend on the initial values) similar to the MHD case [27].

7.1.1. Scaling laws. We choose $z(r)$ so that $\nu(r)$ remains fixed at the initial value ν_0 [13]. Then from equation (28)

$$z(r) = 2 - A_d g(r) - M_d f(r). \tag{44}$$

Furthermore, from the rescaled viscosity, we get the scaling relation for the renormalized viscosity as

$$\nu_R(k, \omega|g_0, f_0, \kappa_0) = \mathrm{e}^{2r-\rho(r)}\nu_R(k\,\mathrm{e}^r, \omega\,\mathrm{e}^{\rho(r)}|g(r), f(r), \kappa(r)) \tag{45}$$

(where $\mathrm{d}\rho/\mathrm{d}r = 2$) and a similar relation for the renormalized diffusivity $\mu_R(k, \omega|g_0, f_0, \kappa_0)$.

From this scaling relation, we can find $\nu_R(k, 0)$ in the RG limit of small k by choosing a large value or r (namely r^*), where $k = \Lambda\,\mathrm{e}^{-r^*}$ and $\rho'(r^*) = z^*$, so that we can write

$$\nu_R(k, 0|g_0, f_0, \kappa_0) = \left(\frac{k}{\Lambda}\right)^{-(2-z^*)} \nu_R(\Lambda, 0|g^*, f^*, \kappa^*) \tag{46}$$

as we approach the fixed point (g^*, f^*, κ^*). A similar relation follows for $\mu_R(k, 0)$.

The spectra $E(k)$ and $C(k)$, given by

$$\frac{1}{2}\langle \boldsymbol{u}^2(\boldsymbol{x},t)\rangle = \int_0^\infty E(k)\,\mathrm{d}k \qquad \text{and} \qquad \langle \psi^2(\boldsymbol{x},t)\rangle = \int_0^\infty C(k)\,\mathrm{d}k$$

can be obtained from

$$E(k) \sim k^{d-1}\int_{-\infty}^{\infty}\frac{\mathrm{d}\omega}{[2\pi]}|G_R(k,\omega)|^2 F(k) \tag{47}$$

and

$$C(k) \sim k^{d-1}\int_{-\infty}^{\infty}\frac{\mathrm{d}\omega}{[2\pi]}|\mathcal{G}_R(k,\omega)|^2 \Theta(k) \tag{48}$$

where

$$G_R(k,\omega) = \frac{1}{-\mathrm{i}\omega + \nu_R(k,0)k^2} \qquad \text{and} \qquad \mathcal{G}_R(k,\omega) = \frac{1}{-\mathrm{i}\omega + \mu_R(k,0)k^2} \tag{49}$$

so that

$$E(k) \sim \frac{k^{d-3-s}}{\nu_R(k,0)} \sim \frac{k^{1-y}}{\nu_R(k,0)} \tag{50}$$

and

$$C(k) \sim \frac{k^{d-3-s'}}{\mu_R(k,0)} \sim \frac{k^{-1-y'}}{\mu_R(k,0)}. \tag{51}$$

Now we shall find these spectra corresponding to the three cases of the passive regime.

Case III. $y < 0$. In this case the stable fixed point is $g^* = 0$, $f^* = 0$, and κ^* is a non-universal constant. Consequently, from equation (44)

$$z^* = 2$$

and hence from equation (46)

$$\nu_R(k,0) \sim \mu_R(k,0) \sim k^0. \tag{52}$$

From equations (50) and (51) this leads to

$$E(k) \sim k^{1-y} \qquad \text{and} \qquad C(k) \sim k^{-1-y'}.$$

As we have noted earlier, this fixed point is stable only when $y' < 0$. Thus, both y and y' need to be negative in this case. Furthermore, for the model we are considering, $y < 2-d$ and $y' > -d$.

Case II. $y = 0$. This marginal case needs exact integration of the flow equations. However, because of the complexity of the flow equations in the case of an active scalar, it is not possible to do this evaluation analytically.

We, however, expect that as we approach the stable fixed point $g^* = 0$ (as discussed earlier, the approach of $g(r)$ towards zero is rather slow in this case), $f^* = 0$, and κ^* is a universal constant, we obtain the same small-k limit of Forster *et al* [13]:

$$\nu_R(k,0) \sim \mu_R(k,0) \sim \left(\ln\frac{\Lambda}{k}\right)^{1/3}. \tag{53}$$

The corresponding spectra, because $y = 0$, are given by

$$E(k) \sim k\left(\ln\frac{\Lambda}{k}\right)^{-1/3} \qquad \text{and} \qquad C(k) \sim k^{-1-y'}\left(\ln\frac{\Lambda}{k}\right)^{-1/3}.$$

As analysed earlier, the stability of these spectra requires $y' < 0$.

Case I. $y > 0$. Now the stable fixed point is $g^* = y/3A_d$, $f^* = 0$, and κ^* is the same universal constant as in case II. Correspondingly, from equation (44)

$$z^* = 2 - \frac{y}{3}$$

and therefore

$$\nu_R(k, 0) \sim \mu_R(k, 0) \sim k^{-y/3}. \tag{54}$$

The spectra are then obtained from equations (50) and (51) as

$$E(k) \sim k^{1-2y/3} \qquad \text{and} \qquad C(k) \sim k^{-1-y+y'/3}.$$

These spectra, as discussed earlier, are stable for all $y > 0$ and $y' < a_d y$. Furthermore, y', which can be negative, is restricted from below by our choice of model, namely $y' > -d$ corresponding to $s' > -2$.

Kolmogorov spectrum. The Kolmogorov spectra $E(k) \sim k^{-5/3}$ and $C(k) \sim k^{-5/3}$ are obtained for the passive scalar convection corresponding to the above $y > 0$ fixed point when we set $y = 4$ and $y' = 2$. These values assert conserved transport of energy and a mean-square scalar in the inertial range (cf the transfer equations in Ruiz and Nelson's work [24]).

From the stability analysis of the $y > 0$ fixed point, we see therefore that the Kolmogorov spectra are stable (on the IR side, since the fixed point is IR stable) against the back reaction of the concentration gradients on the Navier–Stokes dynamics, in three dimensions. This stability runs smoothly over to infinite dimensions, whereas in the MHD case the Kolmogorov spectrum is marginally stable in infinite dimensions.

Furthermore, we observe that the Kolmogorov spectrum is also stable when we artificially suppress the renormalization of α_0. This situation is quite unlike the MHD case, where without this renormalization the Kolmogorov spectrum will only be marginally stable.

7.2. Active regimes

The fixed point $\kappa = 0$ (with $g/\kappa \to 0$) and $f \neq 0$ is unstable for all dimensions $d \geqslant 2$.

The fixed point $g = 0$, $\kappa \neq 0$, $f \neq 0$ is also unstable.

In $d = 3$, both the fixed points $u \neq 0$, $f \neq 0$, $\kappa = 0$ and $g \neq 0$, $f \neq 0$ and $\kappa^{-1} = 0$ are found to be unstable. Here $u = g/\kappa$.

8. Conclusion

We have found that the stability of the fixed point for passive convection in the presence of the active dynamics depends on both the parameters y and y', which determine the correlations of the stirring fields to the (modified) Navier–Stokes equation and the convection equation, respectively. This is quite unlike the case of pure passive convection, where the stability depends only on y, y' being left as a disposable parameter (as far as stability is concerned).

Furthermore, we see that the active-vertex coupling α_0 undergoes a non-zero correction due to renormalization in the IR limit, which is to be explicitly taken into account, since there is no known invariance principle that does not allow such renormalization. The passive couplings λ_0 and $\bar{\lambda}_0$, on the other hand, do not acquire any renormalization, being necessarily a consequence of Galelian invariance [13].

The renormalization of the active vertex makes the stability of the passive regime dependent also on the dimensionality d, and not simply on y and y'. In three dimensions, we find the criterion of stability for the passive regime as $y' < 1.3917y$ along with $y > 0$. Thus the Kolmogorov spectrum, which occurs for $y = 4$ and $y' = 2$, is stable against the active dynamics.

In infinite dimensions, the criterion for the stability of the passive regime is found to be $y' < 1.333y$, and hence the Kolmogorov case is still stable. This is to be contrasted with the corresponding criterion in the MHD case, where one obtains a marginal stability of the Kolmogorov cascade in infinite dimensions.

Finally, we observe that there is no other stable fixed point which could be associated with the equipartition spectra. We have noticed that the correction to the bare diffusivity at each step of the RG iteration (although positive due to passive convection) is negative due to the active dynamics, which should be associated with the instability of the fixed points in the active regime. A possible reason for such instability would seem to be that the RG seeks a fixed point which is stable in the IR limit, while this (equipartition) regime necessarily belongs to the UV domain, and the existence of this regime requires a locked-in concentration gradient field in the IR domain, according to the Kraichnan phenomenology [10] as described in the introduction. Ruiz and Nelson [24] have in fact shown, from the transfer equations of the EDQNM closure, that taking triad interactions coming from wavenumbers $p \ll q \approx k$ leads to this equipartition. However, the RG takes account of interactions coming from wavenumbers belonging to a different domain of interactions, namely $p \approx q \gg k$.

Acknowledgments

Several discussions with M K Verma are gratefully acknowledged. A part of this work has been supported by a post-doctoral fellowship received by M K Nandy from the Institute of Physics, Bhubaneswar, India.

References

[1] Kolmogorov A N 1941 *C.R. Acad. Sci., URSS* **30** 301
[2] Oboukhov A M 1941 *C.R. Acad. Sci., URSS* **32** 19
[3] Oboukhov A M 1949 *Izv. Akad. Nauk, SSSR, Geogr. i. Geofiz.* **13** 58
[4] Corrsin S 1951 *J. Appl. Phys.* **22** 469
[5] Batchelor G K 1959 *J. Fluid Mech.* **5** 113
[6] Kraichnan R H 1959 *J. Fluid Mech.* **5** 497
[7] Wyld H W 1961 *Ann. Phys., NY* **14** 143
[8] Edwards S F 1964 *J. Fluid Mech.* **18** 239
[9] Martin P C, Siggia E D and Rose H A 1973 *Phys. Rev.* A **8** 423
[10] Kraichnan R H 1965 *Phys. Fluids* **8** 575
Kraichnan R H 1965 *Phys. Fluids* **8** 995
[11] Kraichnan R H 1966 *Phys. Fluids* **9** 1728
[12] Leslie D C 1973 *Developments in the Theory of Turbulence* (Oxford: Clarendon)
[13] Forster D, Nelson D R and Stephen M J 1977 *Phys. Rev.* A **16** 732
[14] Ma S K and Mazenko G 1975 *Phys. Rev.* B **11** 4077
[15] DeDominicis C and Martin P C 1979 *Phys. Rev.* A **19** 419
[16] Yakhot V and Orszag S A 1986 *J. Sci. Comput.* **1** 3
[17] Bhattacharjee J K 1988 *J. Phys. A: Math. Gen.* **21** L551
[18] Bhattacharjee J K 1989 *Phys. Rev.* A **40** 6374
[19] Bhattacharjee J K 1991 *Phys. Fluids* A **3** 879
[20] Nandy M K and Bhattacharjee J K 1991 *Phys. Lett.* **152A** 281

[21] Nandy M K and Bhattacharjee J K 1995 *Int. J. Mod. Phys.* B **9** 1081
[22] Bhattacharjee J K and Ferrell R A 1981 *Phys. Rev.* A **23** 1511
[23] Olochowy G and Sengers J V 1988 *Phys. Rev. Lett.* **61** 15
[24] Ruiz R and Nelson D R 1981 *Phys. Rev.* A **23** 3224
[25] Pouquet A 1978 *J. Fluid Mech.* **88** 1
[26] Pouquet A, Frisch U and Léorat J 1976 *J. Fluid Mech.* **77** 321
[27] Fournier J-D, Sulem P-L and Pouquet A 1982 *J. Phys. A: Math. Gen.* **15** 1393–420
[28] Mou C Y and Weichman P B 1993 *Phys. Rev. Lett.* **70** 1101
Mou C Y and Weichman P B 1995 *Phys. Rev.* E **52** 3738–96